AAPT PHYSICS EDUCATION | AMERICAN JOURNAL of PHYSICS

The Sagnac effect and pure geometry

Angelo Tartaglia and Matteo Luca Ruggiero

Citation: American Journal of Physics **83**, 427 (2015); doi: 10.1119/1.4904319
View online: http://dx.doi.org/10.1119/1.4904319
View Table of Contents: http://scitation.aip.org/content/aapt/journal/ajp/83/5?ver=pdfcov
Published by the American Association of Physics Teachers

The Sagnac effect and pure geometry

Angelo Tartaglia[a] and Matteo Luca Ruggiero
DISAT, Politecnico di Torino, Corso Duca degli Abruzzi 24, Torino, Italy and INFN, Sezione di Torino, Via Pietro Giuria 1, Torino, Italy

(Received 24 July 2014; accepted 2 December 2014)

The Sagnac effect is usually deemed to be a special-relativistic effect produced in an interferometer when the device is rotating. Two light beams traveling around the interferometer in opposite directions require different times of flight to complete their closed path, giving rise to a phase shift proportional to the angular velocity of the apparatus. Here, we show that the same result can be obtained in the absence of rotation, when there is relative motion (be it inertial or not) between the source/receiver of light and the interferometer. Our argument will use both a simple algebraic analysis and a plain geometric approach in flat spacetime. We present an explicit example to illustrate our point and briefly discuss other apparently correct interpretations of the Sagnac effect, including an analogy to the Aharonov-Bohm effect. Finally, we sketch a possible application of the non-rotational Sagnac effect.
[http://dx.doi.org/10.1119/1.4904319]

I. INTRODUCTION

The Sagnac effect takes its name from Georges Marc Marie Sagnac, a French physicist who, in 1913, partially interpreting previous experimental evidence, showed that the time of flight of light emitted by a source on a rotating platform and sent back by means of mirrors along a closed path was asymmetric, depending on the direction that the light travels around the apparatus. A simplified diagram of Sagnac's experiment is shown in Fig. 1. The difference in time of flight between the forward (in the sense of rotation) and backward beams is proportional to the angular velocity of the platform and appears as a phase difference measured by an interferometer. Sagnac interpreted this result as evidence *against* Einstein's relativity and in favor of a static luminiferous ether.[1,2] It was, however, immediately and easily shown that the Sagnac effect is a fully relativistic effect.

Today, the Sagnac effect is relevant for various applications, all related to the measurement of rotation rates. On the commercial side we have *gyrolasers*,[3] developed since the 1970s, used on planes, ships, submarines, and missile guidance systems. The name "gyrolaser" is motivated by the fact that the devices replace old mechanical gyroscopes and use a laser to produce the counter-rotating light beams. Instead of exploiting the interference between the two opposed light rays, they measure the beat frequency of the standing wave resulting from the superposition of two waves propagating in opposite directions; that frequency is again proportional to the absolute angular velocity of the apparatus.

The most sensitive gyrolasers, or *ring lasers*, are used for high-accuracy geophysical measurements.[4] They sense the diurnal rotation of the Earth, the wobbles of the terrestrial axis, and tiny rotations of the laboratory hosting the instrument, due to elastic deformations of the ground caused by liquid and solid tides and also by various surface phenomena.

The extremely high sensitivity obtained in recent ring lasers is such that the Sagnac effect is now also becoming important for fundamental physics. The possibility has been suggested of using large ring lasers to detect the Lense-Thirring effect of general relativity on Earth,[5] and an experiment, which goes by the acronym GINGER, is now in the development and preliminary testing phase at the National Laboratories of the Italian INFN at the Gran Sasso site.[6,7]

The Sagnac effect also plays a role in the use of Global Positioning System (GPS) signals to determine the position of a receiver. A Sagnac correction is required because a rotating clock (onboard a satellite or on the surface of the Earth) loses synchronization with itself at each turn. The relevance of the relativistic effects on clocks carried around the Earth, either in the same or in the opposite sense with respect to Earth's rotation, was experimentally verified by Hafele and Keating.[8–10]

The Sagnac effect has been deeply investigated, ever since Sagnac's experiments, as a probe of the theory of relativity and, more recently, in connection with the issue of synchronization in rotating reference frames.[11,12] All of this work is well known, but it is often accompanied by a feeling that the Sagnac effect is essentially due to the presence of a rotating observer or rotating device: in short, to non-inertial motion.

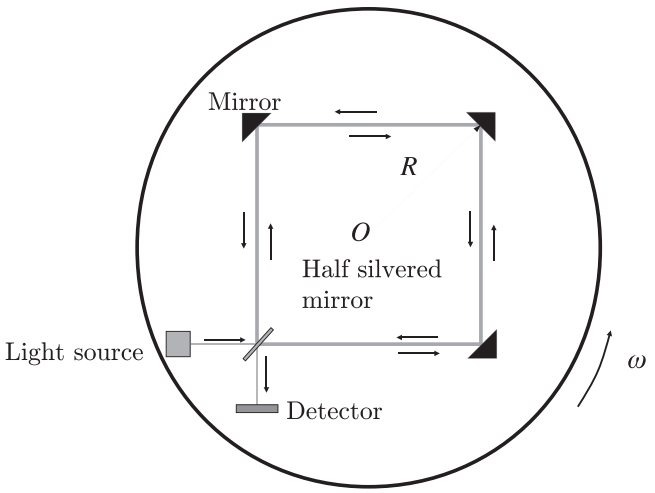

Fig. 1. Basic scheme of the Sagnac interferometric experiment. There is a turntable rotating at angular speed ω. The table carries a light source, a half-silvered mirror, three more mirrors, and a detector where the interference pattern is visible. The total length of the square path is ℓ. The arrows show the directions of the light beams.

In reality, however, non-inertial motion is not necessary, and examples of papers elaborating on various aspects of the Sagnac effect, without discussing the necessity of rotation, are Refs. 13–15. Indeed, a few years ago some experimental papers were published that claim that even if no rotation is present, a "generalized Sagnac effect" arises in a uniformly moving fiber.[16,17] In the present paper, we aim at addressing this issue. That is, we show that the real ingredients of the Sagnac effect are: (1) a closed circuit followed by light in opposite directions; and (2) a relative (even inertial) motion of the emitter/receiver with respect to the physical apparatus supporting the closed light path. We believe that this approach could be useful in teaching the foundations of relativity because the calculations involved are simple and because they allow a deep insight into the physics of the problem (which ultimately is connected with the relativity of simultaneity).

II. THE SAGNAC EFFECT

The physical principles of the Sagnac effect are explained in full detail in the well-known paper by Post;[18] they can be summarized as follows.

The Sagnac effect can easily be described in classical terms if one assumes that the speed of light is c with respect to a static ether. For the rotating platform described in the Introduction, one can see that if the light is going around the device in the same direction as the rotation, then it will take longer for it to reach the emission point because, meanwhile, the receiver will have moved forward by a distance $\Delta\ell_+ = vt_+$, where t_+ is the total time of flight and v is the velocity of the emitter with respect to the ether; the geometric length of the path is ℓ. Hence, the time of flight is read from the following relation $(\ell + \Delta\ell_+)/c = \Delta\ \ell_+/v$. For light going around in the opposite sense, the receiver will move towards the returning beam so that the path will be shorter by $\Delta\ell_- = vt_-$, whence $(\ell - \Delta\ell_-)/c = \Delta\ell_-/v$. Solving for t_+ and t_- gives the time of flight difference:

$$\Delta t = t_+ - t_- = \frac{2\ell v}{c^2 - v^2}. \tag{1}$$

An equivalent deduction can be made adopting the viewpoint of the rotating observer. In the observer's reference frame, light will be expected to have speed $c - v$ in one direction (forward) and $c + v$ in the other; now the path length is the same ℓ for both (see Fig. 1). The times of flight are again different and a trivial calculation reproduces Eq. (1).

It is useful to rewrite Eq. (1) in terms of the angular velocity ω of the platform. If R is the distance of the emitter/detector from the rotation axis, then we have $v = \omega R$. We simplify the geometry by assuming that the light path is a circle[19] at radius R, so that $\ell = 2\pi R$. Considering that in all practical cases $v \ll c$, Eq. (1) can be written as

$$\Delta t \approx 4\frac{\mathbf{A}\cdot\boldsymbol{\omega}}{c^2}. \tag{2}$$

Here $\mathbf{A}$ is a vector whose magnitude is equal to the area enclosed by the path of the light beams (πR^2) and is oriented perpendicular to the plane of the trajectory,[20] while $\boldsymbol{\omega}$ is the (vector) angular velocity; the dot product projects the area into the plane of rotation. Equation (2) is the famous Sagnac formula, where the $\approx$ symbol is usually replaced by an equals sign, although the approximation is still present.

As mentioned above, however, the Sagnac effect does not depend on the existence of the ether. Special (or general) relativity is essentially geometry, so we can use a geometric approach to work out what happens. In the simplified configuration of a circular light trajectory, the situation can be represented in the spacetime graph shown in Fig. 2.

Everything is drawn on the surface of a cylinder and the viewpoint is that of an inertial observer at rest with respect to the axis of the rotating platform.[21] The vertical axis of the figure is *not* the rotation axis of the turntable; it is the coordinate time axis. The worldline of the rotating observer is a helix and the two light beams are represented by two opposite helices as well, which, after one turn, intersect the worldline of the observer at two different events, labeled A and B. The interval between A and B is the proper time difference measured by the observer between the arrival times of the two light rays.

A cylinder is a flat surface, so we can obtain a simpler view by cutting the cylinder along one generatrix and opening it into a flat spacetime strip as shown in Fig. 3. In this figure, the helices become straight lines and the geometry is clear; the only trick is to remember that the right border of the strip is identified with the left border, so that lines reaching one border reappear at the corresponding point on the other.

The properties of straight lines and triangles in Fig. 3 are the usual ones, except that this is not Euclidean space, but Minkowski spacetime, with coordinate time on the y-axis and position on the x-axis. Thus, the squared length of a hypotenuse in this geometry is a squared proper time multiplied by c^2 and is given by the *difference* between the squared

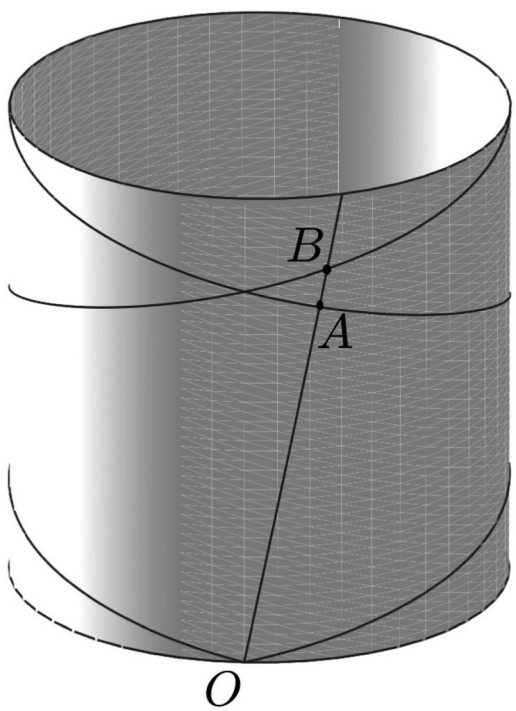

Fig. 2. Spacetime diagram of the Sagnac effect. Line OAB is the world line of the rotating observer. The line is a helix drawn on a three-dimensional cylinder. Inertial time is measured along the vertical axis. The other two lines (helices) represent two light rays. Events A and B are where the observer is reached by the counter- and co-rotating beams, respectively.

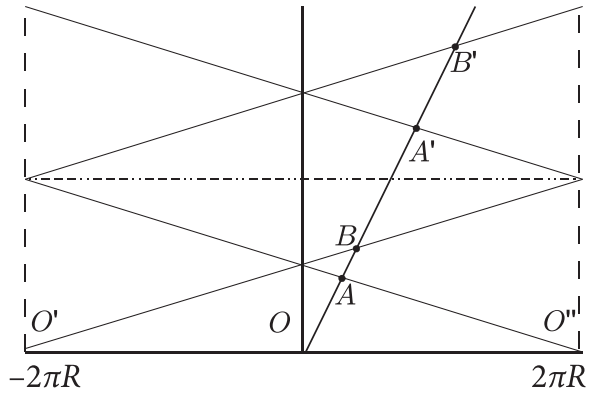

Fig. 3. Another depiction of the events of Fig. 2. The cylinder has been cut along a generatrix passing through the rotating observer at time 0 and opened. For convenience, two replicas of the opened cylinder are shown side by side: one unrolled to the right, the other to the left, with each light ray shown only where needed for the geometric construction. Points O' and O'' coincide with O. The vertical straight line is the world line of an inertial observer at rest with respect to the axis of the disk. Segment AB indicates the Sagnac effect as measured by the rotating observer.

coordinate time span (times c^2) and the square of the traveled distance. A purely geometrical argument,[21] applied to Fig. 3, leads again, to lowest order in v/c, to Eq. (2).

If one prefers to proceed analytically, the starting point can be the line element of Minkowski spacetime written using cylindrical coordinates in space: $ds^2 = c^2dt^2 - dr^2 - r^2d\phi^2 - dz^2$. Introducing the constraints $r = R = \text{constant}$ and $z = \text{constant}$, corresponding to all physics taking place on the rim of a disk perpendicular to the z-axis, the problem is reduced to two effective dimensions and the line element becomes

$$ds^2 = c^2dt_0^2 - R^2d\phi_0^2. \tag{3}$$

The subscript 0 here means that the coordinates are those of the inertial observer.

To account for the rotation of the platform, it is convenient to introduce axes rotating together with the platform so that the angular coordinate becomes $\phi = \phi_0 - \omega t_0$. Then, we need a Lorentz transformation between the inertial observer at rest with the axis of the platform and the inertial frame instantaneously comoving with the observer on the rim of the turntable. Lorentz transformations leave the line element unchanged, so that in the rotating reference frame it becomes

$$ds^2 = (c^2 - \omega^2R^2)dt^2 - R^2d\phi^2 - 2R^2\omega\, d\phi\, dt. \tag{4}$$

On writing the previous expression in the form

$$ds^2 = g_{00}\, dt^2 + g_{\phi\phi}\, d\phi^2 + 2g_{0\phi}\, dt\, d\phi, \tag{5}$$

and considering that for light we have $ds = 0$, we can solve for dt:

$$dt = \frac{-g_{0\phi}d\phi \pm \sqrt{g_{0\phi}^2\, d\phi^2 - g_{\phi\phi}g_{00}\, d\phi^2}}{g_{00}}. \tag{6}$$

We are interested in solutions located in the future, so we choose $dt > 0$, i.e., the + sign in Eq. (6). Under the simplified assumption that light moves along a circumference, if we integrate in the two opposite directions (counterclockwise with $d\phi > 0$ and clockwise with $d\phi < 0$) from the emission to the absorption events, we get the expression for the co-rotating (t_+) and counter-rotating (t_-) times of flight, and the difference between them turns out to be

$$\Delta t = t_+ - t_- = -2\oint_\ell \frac{g_{0\phi}}{g_{00}} R\, d\phi, \tag{7}$$

where ℓ is the circumference of a circle of radius R.[22] Moreover, the observer measures the proper-time difference

$$\Delta\tau = -2\sqrt{g_{00}}\oint_\ell \frac{g_{0\phi}}{g_{00}} R\, d\phi. \tag{8}$$

On substituting the explicit expressions in Eq. (4) for the metric coefficients, we obtain the following formulas for the coordinate and proper time-of-flight differences:

$$\Delta t = 4\frac{\pi R^2\omega}{c^2(1 - \omega^2R^2/c^2)}, \tag{9}$$

$$\Delta\tau = 4\frac{\pi R^2\omega}{c^2\sqrt{1 - \omega^2R^2/c^2}}. \tag{10}$$

At the lowest approximation order in $\omega R/c$ these two expressions coincide, and they are in agreement with Eq. (2), with $\mathbf{A} = \pi R^2\hat{\mathbf{u}}_z$, where the unit vector $\hat{\mathbf{u}}_z$ points along the z direction.

III. SAGNAC WITHOUT ROTATION

Despite the widespread tendency to ascribe the Sagnac effect to rotating systems, it is easy to show that rotation is not essential. Consider a source/receiver of light in inertial motion at speed v with respect to a set of mirrors rigidly fastened to one another or to an optical fiber so that they guide the light beams emitted by the moving source along a closed path in space. The situation is schematically illustrated in Fig. 4, where an optical fiber is envisaged.

Repeating the simple reasoning made at the beginning of Sec. II, we again arrive at the same result as in Eq. (1). The only additional clarification is that Eq. (1) is expressed from the viewpoint of an observer at rest with respect to the fiber (or array of mirrors); for the proper time measured by the

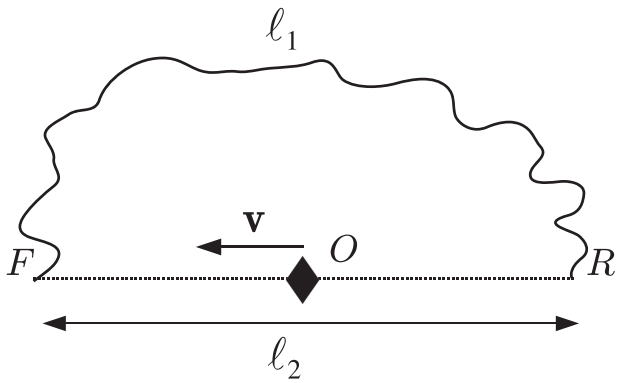

Fig. 4. Object O (◆) represents a source/receiver of light moving with velocity $\mathbf{v}$. Light is sent both forward and backward (dashed lines). The irregular line joining F with R represents an optical fiber of length ℓ_1, along which the light travels. Observer O is moving with velocity v with respect to the fiber. The total length of the path is $\ell = \ell_1 + \ell_2$.

moving emitter/receiver we would instead have (with $\beta = v/c$)

$$\Delta\tau = 2\frac{\ell v}{c^2\sqrt{1-\beta^2}} \approx 2\frac{\ell v}{c^2}. \tag{11}$$

No rotation, acceleration, or enclosed area appears in this expression. What matters is just the existence of relative (even inertial) motion and of a closed path in space. Of course, with reference to Fig. 4, the velocity **v** is parallel to the light rays along the path *RF*.

The effect we have just described and the related formula (11) have been experimentally verified by Wang, Zheng, Yao, and Langley (WZYL).[16,17]

Using the geometrical approach, this result is rather obvious. In spacetime, the world lines are drawn again on a (non-circular) cylinder. The only difference is that in Fig. 2 the cylinder had a circular cross section, while now the cross section is irregular. In either case, the cylinder is a flat bidimensional Minkowski surface and, when opening it into a plane, the graph is exactly as in Fig. 3.

It is worth noting that formula (1) also appears in Ref. 24, where it is related to the relativity of simultaneity typical of special relativity.

Another aspect to clarify is related to the form of Eq. (2). The accidental presence of the area A suggested to some people (for instance, Refs. 25 and 26) an interpretation of the Sagnac effect (at least for matter waves) as a sort of Aharonov-Bohm effect. However, this is just an analogy, which holds only at lowest relativistic order (see, e.g., Ref. 23).

IV. A SIMPLE EXAMPLE

In order to obtain deeper insight into the Sagnac effect, let us consider a simple example where the calculation can be carried out in full detail.

Our interferometer is at rest in the laboratory and is made of four mirrors (M_1, M_2, M_3, and M_4) at the corners of a rectangle of width $2a$ and height $2b$. Using Cartesian coordinates, the mirror positions are given in Fig. 5, and the interferometer path length is $\ell = 4a + 4b$. An observer, moving at speed v to the right in the laboratory frame, sends two counter-propagating light signals when he/she is at the origin. The paths of the counterclockwise (CCW) and clockwise (CW) rays are depicted in Figs. 6 and 7, respectively, as seen in the laboratory frame. Note that in the laboratory frame, the CW path is not closed, while the CCW path overlaps with itself. What we want to show, by the following calculation, is that in the frame moving with the observer both paths are closed.

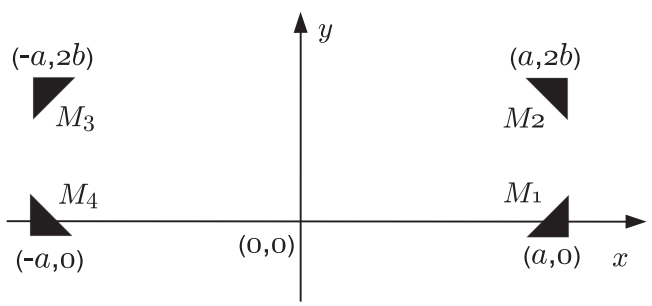

Fig. 5. The four mirrors M_1, M_2, M_3, M_4 that form the interferometer are at rest in the laboratory frame.

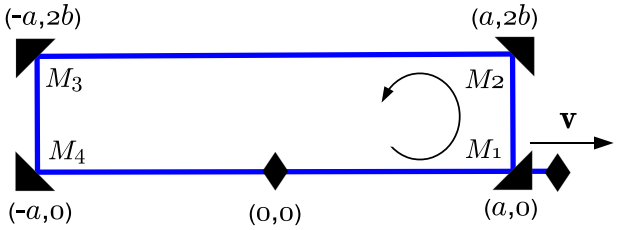

Fig. 6. The path of the CCW light ray, as seen in the laboratory. The symbol ◆ marks the positions of the observer when the signal is sent (left) and received (right). The parameters used are $\beta = 20/101$ (giving $\gamma = 101/99$) and $b = a/4$.

In terms of Cartesian spacetime coordinates (ct, x, y) in the laboratory frame, the event sequence along the CCW path is:

- e_0: (0, 0, 0) (emission)
- e_1: $(a, a, 0)$ (reflection by $M1$)
- e_2: $(a + 2b, a, 2b)$ (reflection by $M2$)
- e_3: $(3a + 2b, -a, 2b)$ (reflection by $M3$)
- e_4: $(3a + 4b, -a, 0)$ (reflection by $M4$)
- e_5: $(ct_1, vt_1, 0) = (4(a+b)/(1-\beta), 4(a+b)\beta/(1-\beta), 0)$ (reception)

In particular, the total propagation time is obtained from $ct_1 = vt_1 + 4a + 4b$.

For the CW path, we have the following events:

- e_0: (0, 0, 0) (emission)
- E_1: $(a, -a, 0)$ (reflection by $M4$)
- E_2: $(a + 2b, -a, 2b)$ (reflection by $M3$)
- E_3: $(3a + 2b, a, 2b)$ (reflection by $M2$)
- E_4: $(3a + 4b, a, 0)$ (reflection by $M1$)
- E_5: $(ct_2, vt_2, 0) = (4(a+b)/(1+\beta), 4(a+b)\beta/(1+\beta), 0)$ (reception)

Again, the total propagation time is obtained from $ct_2 = 4a + 4b - vt_2$. As expected, the CCW time is longer than the CW time, since $t_1 > t_2$, so the two signals reach the observer at different times.

To obtain the coordinates of these events in the frame co-moving with the observer, we use the Lorentz transformations:

$$ct' = \gamma(ct - \beta x), \quad x' = \gamma(x - \beta ct), \quad y' = y, \tag{12}$$

where $\gamma = (1-\beta^2)^{-1/2}$. As a consequence, the Cartesian coordinates (ct', x', y') of the events for the CCW path are

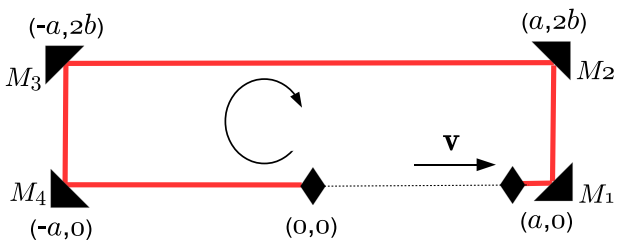

Fig. 7. The path of the CW light ray, as seen in the laboratory. The symbol ◆ marks the positions of the observer when the signal is sent (left) and received (right). The parameters used are $\beta = 20/101$ (giving $\gamma = 101/99$) and $b = a/4$.

- e_0: (0, 0, 0) (emission)
- e_1: $(\gamma(1-\beta)a, \gamma(1-\beta)a, 0)$ (reflection by $M1$)
- e_2: $(\gamma(1-\beta)a + 2\gamma b, \gamma(1-\beta)a - 2\gamma\beta b, 2b)$ (reflection by $M2$)
- e_3: $(\gamma(3+\beta)a + 2\gamma b, -\gamma(1+3\beta)a - 2\gamma\beta b, 2b)$ (reflection by $M3$)
- e_4: $(\gamma(3+\beta)a + 4\gamma b, -\gamma(1+3\beta)a - 4\gamma\beta b, 0)$ (reflection by $M4$)
- e_5: $(4\gamma(1+\beta)(a+b), 0, 0)$ (reception)

For the CW path, we have the following coordinates:

- e_0: (0, 0, 0) (emission)
- E_1: $(\gamma(1+\beta)a, -\gamma(1+\beta)a, 0)$ (reflection by $M4$)
- E_2: $(\gamma(1+\beta)a + 2\gamma b, -\gamma(1+\beta)a - 2\gamma\beta b, 2b)$ (reflection by $M3$)
- E_3: $(\gamma(3-\beta)a + 2\gamma b, \gamma(1-3\beta)a - 2\gamma\beta b, 2b)$ (reflection by $M2$)
- E_4: $(\gamma(3-\beta)a + 4\gamma b, \gamma(1-3\beta)a - 4\gamma\beta b, 0)$ (reflection by $M1$)
- E_5: $(4\gamma(1-\beta)(a+b), 0, 0)$ (reception)

These collections of event coordinates show that in the moving frame the two paths are closed. In particular, the CCW path is a polygon whose vertices have the following (x', y') coordinates: $(0,0)$, $(\gamma(1-\beta)a, 0)$, $(\gamma(1-\beta)a - 2\gamma\beta b, 2b)$, $(-\gamma(1+3\beta)a - 2\gamma\beta b, 2b)$, $(-\gamma(1+3\beta)a - 4\gamma\beta b, 0)$. The shape of this polygon is depicted in Fig. 8, and its perimeter is given by $\ell_1 = 4\gamma(1+\beta)(a+b)$. Since the traversal time is given from event e_5 as $t'_1 = 4\gamma(1+\beta)(a+b)/c$, we see that the average traversal speed is $\ell_1/t'_1 = c$.

On the other hand, the CW path is a polygon whose vertices have the following coordinates: $(0,0)$, $(-\gamma(1+\beta)a, 0)$, $(-\gamma(1+\beta)a - 2\gamma\beta b, 2b)$, $(\gamma(1-3\beta)a - 2\gamma\beta b, 2b)$, $(\gamma(1-\beta)a - 4\gamma\beta b, 0)$. The shape of this polygon is depicted in Fig. 9, and its perimeter is given by $\ell_2 = 4\gamma(1-\beta)(a+b)$. Again, by reading the traversal time $t'_2 = 4\gamma(1-\beta)(a+b)/c$ from E_5, we see that the average traversal speed is $\ell_2/t'_2 = c$.

We remark that we can easily explain the tilt of the lateral edges in Figs. 8 and 9 in terms of the motion of the observer. Indeed, when the light ray moves upward at right angles to the x-axis in the laboratory frame, it has to move upward and *left* in the observer's frame. Similarly, when it moves downward, it has to move downward and *left* in the observer's frame.

The moving observer measures a proper time difference between the propagation of the CCW and CW rays given by

$$\Delta\tau = t'_1 - t'_2 = 8\gamma\frac{(a+b)}{c}\beta \approx 2\frac{\ell v}{c^2}. \tag{13}$$

This result is in agreement with the general formula (11). Moreover, this calculation helps us understand the origin of the time difference arising in the moving frame: the two light paths, which are congruent except for their end pieces in the laboratory frame, are no longer congruent in the observer's moving frame. Consequently, because these paths have different lengths, light must take different amounts of time to propagate around the paths.

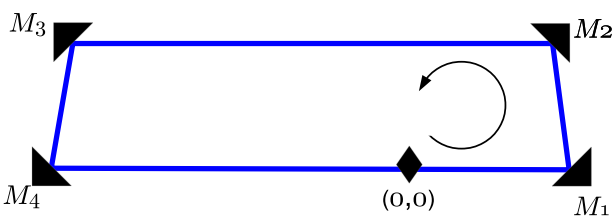

Fig. 8. The path of the CCW light ray, as seen in the observer's frame. Both emission and reception take place at the origin (0, 0). The parameters used are $\beta = 20/101$ (giving $\gamma = 101/99$) and $b = a/4$.

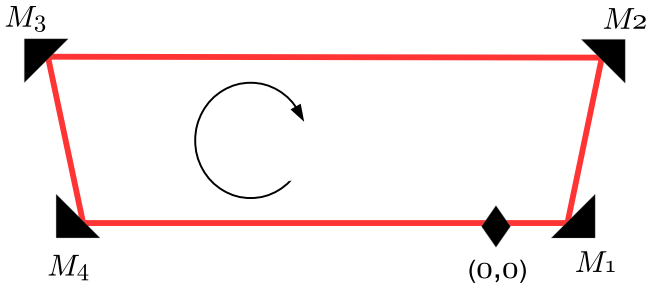

Fig. 9. The path of the CW light ray, as seen in the observer's frame. Both emission and reception take place at the origin (0, 0). The parameters used are $\beta = 20/101$ (giving $\gamma = 101/99$) and $b = a/4$.

This example shows how to explain the Sagnac effect in the case of an inertial observer, but a similar approach can be used to do the same thing for an accelerated one. However, while in our case, the observer's space is Euclidean and everything is unambiguous, care is needed in defining the spatial geometry for an arbitrary accelerated observer. Spatial geometry can be defined in terms of congruence of world lines (see, e.g., Ref. 27), so it is not simply related to *one* observer but rather depends on a *collection* of observers.

Things are simple in the case of the uniformly rotating disk, where the ordinary Sagnac effect is usually explained. A natural choice of observers that allows us to define the spatial geometry is given by the observers sitting at fixed points on the disk (see, again, Refs. 27 and 28). In this case, both the co-rotating and the counter-rotating rays propagate along the *same curve*, and the Sagnac effect can be explained in terms of different speeds of light in the co-rotating and counter-rotating directions, if clocks along the rim of the disk are Einstein-synchronized, or in terms of a time gap, if a different synchronization procedure is used (see, e.g., Refs. 15 and 29).

V. POSSIBLE APPLICATIONS

Aside from the conceptual aspects, the phenomenon we have interpreted and WZYL have measured prompts some possible interesting applications, as suggested in Ref. 17.

As we see from Eq. (11), the time-of-flight difference for light is proportional to the relative velocity of the source with respect to the fiber or the mirrors. Now, consider a ring laser where the active segment is not rigidly connected to the rest of the annular cavity; imagine, for instance, that the active cavity is attached to the rest via an elastic support allowing for relative vibrations. What is usually measured in a ring laser is a beat frequency of two counter-propagating beams. The beat frequency is easily obtained from Eq. (11) and is given by

$$\nu_b = \frac{v}{\lambda}, \tag{14}$$

where λ is the wavelength of the laser. Here, we have a simple speedometer for instantaneous velocities, where 1 m/s

corresponds roughly to beat frequencies on the order of MHz. In the obvious case that the active element is subject to an acceleration, a simple differentiation of the output converts the device into an accelerometer. Of course practical analyses on the stability of the laser modes should be made, but the idea is appealing.

VI. CONCLUSION

We have shown that the Sagnac effect is due to the closure of the path followed by light and to the relative motion of the observer with respect to the physical system that causes the beam to bend and come back to the observer. After introducing the foundations of the effect, we have studied in full detail a simple example to focus on the origin of the time delay in the inertial frame of the moving observer, and we have made a comparison with the case of the rotating observer. We have proved that the Sagnac effect is not peculiar to rotations and accelerated motion; rather, it originates from the closure of the two space paths as seen in the frame comoving with the emitter/receiver and from relative motion between the emitter/receiver and the mirrors (or physical device). Indeed, its foundations are related to the relativity of simultaneity. On the practical side, one can imagine interesting applications based on the use of ring lasers as linear accelerometers.

ACKNOWLEDGMENTS

The authors are indebted to one of the referees for suggesting the example in Sec. IV.

[a]Author to whom correspondence should be addressed. Electronic mail: angelo.tartaglia@polito.it

[1]Georges Sagnac, "Sur la propagation de la lumière dans un système en translation et sur l'aberration des étoiles," C. R. Acad. Sci. Paris **141**, 1220–1223 (1913).
[2]Georges Sagnac, "L'éther lumineux démontré par l'effet du vent relatif d'éther dans un interféromètre en rotation uniforme," C. R. Acad. Sci. Paris **157**, 708–710 (1913), English translation in *Relativity in Rotating Frames*, edited by G. Rizzi and M. L. Ruggiero (Kluwer, Dordrecht, 2003), pp. 5–7.
[3]W. W. Chow *et al.*, "The ring laser gyro," Rev. Mod. Phys. **57**, 61–104 (1985).
[4]K. U. Schreiber and J.-P. R. Wells, "Large ring lasers for rotation sensing," Rev. Sci. Instrum. **84**, 041101–041101-26 (2013).
[5]G. E. Stedman, K. U. Schreiber, and H. R. Bilger, "On the detectability of the Lense-Thirring field from rotating laboratory masses using ring laser gyroscope interferometers," Class. Quantum Grav. **20**, 2527–2540 (2003).
[6]F. Bosi *et al.*, "Measuring gravitomagnetic effects by a multi-ring-laser gyroscope," Phys. Rev. D **84**, 122002-1–23 (2011).
[7]M. Allegrini *et al.*, "A laser gyroscope system to detect the gravitomagnetic effect on Earth," J. Phys.: Conf. Ser. **375**, 062005-1–6 (2012).
[8]J. C. Hafele and R. E. Keating, "Around-the-world atomic clocks: Predicted relativistic time gains," Science **177**(4044), 166–168 (1972).
[9]J. C. Hafele and R. E. Keating, "Around-the-world atomic clocks: Observed relativistic time gains," Science **177**(4044), 168–170 (1972).
[10]R. Schlegel, "Comments on the Hafele-Keating experiment," Am. J. Phys. **42**, 183–187 (1974).
[11]R. Anderson, H. R. Bilger, and G. E. Stedman, "Sagnac effect: A century of Earth-rotated interferometers," Am. J. Phys. **62**, 975–985 (1994).
[12]*Relativity in Rotating Frames*, edited by G. Rizzi and M. L. Ruggiero (Kluwer, Dordrecht, 2003).
[13]A. Zajac, H. Sadowski, and S. Licht, "Real fringes in the Sagnac and Michelson interferometers," Am. J. Phys. **29**, 669–673 (1961).
[14]G. C. Babcock, "The Sagnac interferometer," Am. J. Phys. **30**, 311 (1962).
[15]K. Kassner, "Ways to resolve Selleri's paradox," Am. J. Phys. **80**, 1061–1066 (2012).
[16]R. Wang, Y. Zheng, A. Yao, and D. Langley, "Modified Sagnac experiment for measuring travel-time difference between counter-propagating light beams in a uniformly moving fiber," Phys. Lett. A **312**, 7–10 (2003).
[17]R. Wang, Y. Zheng, and A. Yao, "Generalized Sagnac effect," Phys. Rev. Lett. **93**, 143901-1–3 (2004).
[18]E. J. Post, "Sagnac effect," Rev. Mod. Phys. **39**, 475–493 (1967).
[19]This would have been practically impossible in Sagnac's time but is feasible today with modern optical fibers, as it is done in commercial gyrolasers.
[20]Actually the planarity is not needed.
[21]A. Tartaglia, "Geometric treatment of the gravitomagnetic clock effect," Gen. Relativ. Grav. **32**, 1745–1756 (2000).
[22]In the most general case ℓ is the integration path and, using arbitrary coordinates, the formula would be $\Delta t = -2\oint_\ell (g_{0i}/g_{00})dx^i$ (see, e.g., Ref. 23).
[23]M. L. Ruggiero and A. Tartaglia, "A note on the Sagnac effect and current terrestrial experiments," Eur. Phys. J. Plus **129**, 126-1–126-5 (2014).
[24]N. Ashby, "The Sagnac effect in the GPS," in *Relativity in Rotating Frames*, edited by G. Rizzi and M. L. Ruggiero (Kluwer, Dordrecht, 2003), pp. 11–28.
[25]G. E. Stedman, "Ring-laser tests of fundamental physics and geophysics," Rep. Prog. Phys. **60**, 615–688 (1997).
[26]E. G. Harris, "The gravitational Aharonov Bohm effect with photons," Am. J. Phys. **64**, 378–383 (1996).
[27]G. Rizzi and M. L. Ruggiero, "Space geometry of rotating platforms: An operational approach," Found. Phys. **32**, 1525–1556 (2002).
[28]K. Kassner, "Spatial geometry of the rotating disk and its non-rotating counterpart," Am. J. Phys. **80**, 772–781 (2012).
[29]G. Rizzi, M. L. Ruggiero, and A. Serafini, "Synchronization Gauges and the principles of special relativity," Found. Phys. **34**, 1835–1887 (2005).